

## Mental rotation and object categorization share a common network of prefrontal and dorsal and ventral regions of posterior cortex

Haline E. Schendan<sup>a,c,d,\*</sup> and Chantal E. Stern<sup>b,c,d</sup>

<sup>a</sup>Department of Psychology, Tufts University, 490 Boston Avenue, Medford, MA 02155, USA

<sup>b</sup>Center for Memory and Brain, Department of Psychology, Boston University, Boston, MA 02215, USA

<sup>c</sup>Department of Psychology, Boston University, Boston, MA 02215, USA

<sup>d</sup>Athinoula A. Martinos Center for Biomedical Imaging, Department of Radiology, Massachusetts General Hospital, Charlestown, MA 02129, USA

Received 4 December 2006; revised 6 January 2007; accepted 14 January 2007

Available online 27 January 2007

The multiple-views-plus-transformation variant of object model verification theories predicts that parietal regions that are critical for mental rotation contribute to visual object cognition. Some neuroimaging studies have shown that the intraparietal sulcus region is critically involved in mental rotation. Other studies indicate that both ventral and dorsal posterior regions are object-sensitive and involved in object perception and categorization tasks. However, it is unknown whether dorsal object-sensitive areas overlap with regions recruited for object mental rotation. Functional magnetic resonance imaging was used to test this directly. Participants performed standard tasks of object categorization, mental rotation, and eye movements. Results provided clear support for the prediction, demonstrating overlap between dorsal object-sensitive regions in ventral–caudal intraparietal sulcus (vcIPS) and an adjacent dorsal occipital area and the regions that are activated during mental rotation but not during saccades. In addition, object mental rotation (but not saccades) activated object-sensitive areas in lateral dorsal occipitotemporal cortex (DOT), and both mental rotation and object categorization recruited ventrolateral prefrontal cortex areas implicated in attention, working memory, and cognitive control. These findings provide clear evidence that a prefrontal–posterior cortical system implicated in mental rotation, including the occipitoparietal regions critical for this spatial task, is recruited during visual object categorization. Altogether, the findings provide a key link in understanding the role of dorsal and ventral visual areas in spatial and object perception and cognition: Regions in occipitoparietal cortex, as well as DOT cortex, have a general role in visual object cognition, supporting not only mental rotation but also categorization. © 2007 Elsevier Inc. All rights reserved.

People are fast and accurate at categorizing objects (e.g., car, dog, or sofa). Numerous theories of visual information processing implicate perceptual and memory functions along the ventral

posterior pathway in object categorization, whereas coordinate system transformations along the dorsal posterior pathway support spatial analysis and action goals (Goodale and Milner, 1992; Ungerleider and Haxby, 1994). However, not only ventral but also dorsal regions of object-sensitive posterior cortex (dorsal foci 1 and 2 [DF1; DF2]) in humans have routinely been observed during object perception and categorization tasks, even under passive viewing (Altmann et al., 2005; Ganis et al., 2007; Grill-Spector et al., 2000, 2001; Hasson et al., 2003). This is consistent with *object model verification* theories of visual cognition, which propose that visual object constancy (i.e., similar task performance under diverse viewing conditions, such as under occlusion and differing view-points) is readily achieved because object processing recruits a prefrontal–parietal network that implements model verification processes; these processes help determine the stored structural model in ventral posterior object-sensitive cortex that best accounts for the visual percept (Ganis et al., 2007; Kosslyn et al., 1994; Lowe, 2000). One variant of this theory, the *multiple-views-plus-transformation* (MVPT) account, specifies that objects are categorized based on multiple two-dimensional (2D) view representations in the ventral stream, and visual constancy is achieved by more strongly engaging the parietal regions implicated in the spatial coordinate transformations required for mental rotation (Bülthoff et al., 1995; Tarr and Pinker, 1989). However, it is unknown whether the dorsal object-sensitive regions are the same as the areas recruited for mental rotation. To test this directly, we used functional magnetic resonance imaging (fMRI) to compare brain activity during mental rotation and object categorization. We also compared this activity with eye movement-related activity to evaluate whether occipitoparietal recruitment merely reflected saccades to different parts of the object. Findings from our study provide clear evidence that cortical regions along the dorsal pathway that are critical for mental rotation (and outside areas implicated in saccades) are also recruited during object categorization, a typical ventral stream function.

Neuropsychological evidence and neuroimaging indicate that the posterior intraparietal sulcus (IPS), especially in the right

\* Corresponding author. Department of Psychology, Tufts University, 490 Boston Avenue, Medford, MA 02155, USA.

E-mail address: Haline.E.Schendan@tufts.edu (H.E. Schendan).

Available online on ScienceDirect (www.sciencedirect.com).

hemisphere, is necessary for the object mental rotation function implicated in MVPT (Corballis, 1997; Harris and Miniussi, 2003). The mental rotation task is a well-established spatial cognition paradigm in which participants see two objects in different orientations and decide whether they are either identical to each other (“same” objects) or left–right mirror images of each other (“different” objects). Response time and decision errors increase linearly as the difference in orientation between the two objects increases. This linear relation is interpreted as evidence that, during mental rotation, observers imagine an object moving through space along the same continuous trajectory as if they were physically rotating it (Shepard and Cooper, 1982). Neuroimaging studies with a parametric design reveal a linear increase in activation of the IPS and adjacent dorsal occipital cortex, especially in the right hemisphere, as the degree of rotation is increased, implicating this dorsal stream region specifically in the scaling of mental rotation task performance with angular disparity (Carpenter et al., 1999; Harris et al., 2000; Podzebenko et al., 2002).

To date, research investigating a more general role for mental rotation processes in object cognition has used mainly indirect behavioral methods (Tarr, 1995), but the findings from neuropsychology and neuroimaging provide some support. Occipitoparietal damage impairs object categorization. For example, patients with the ‘perceptual categorization deficit’ type of visual apperceptive agnosia (Farah, 1990) have right inferior parietal damage, including the region around IPS and dorsal object-sensitive areas DF1 and DF2, and problems with impoverished images, including fragmented pictures, overlapping drawings, silhouettes, and unusual lighting and views (Turnbull, 1997; Turnbull et al., 1997a; Turnbull and McCarthy, 1996; Warrington, 1982). These ‘unusual views deficit’ patients do well with canonical (i.e., best) or more typical views but are impaired with unusual views of objects. The goal of our fMRI study was to fill this empirical gap by evaluating directly whether regions critical for mental rotation and the dorsal object-sensitive areas overlap.

We acquired fMRI data in the same individuals during three tasks. Standard activation paradigms were used to define mental rotation-related and object-sensitive areas. The mental rotation task used a design and procedures previously validated in neuroimaging studies (Cohen et al., 1996; Kosslyn et al., 1998) and materials from our prior neuropsychological work on mental rotation of objects in-depth (Amick et al., 2006). The object-sensitive paradigm was based on prior research defining object-sensitive areas (Malach et al., 1995), but, instead of passive viewing, participants did a speeded object-decision task, pressing one key as soon as they could identify what the object was and another key if the image was a meaningless texture. Finally, participants did a saccade task with alternating blocks of fixation and eye movements. Results from all three tasks were compared directly. As the MVPT account predicts, results revealed that the dorsal object-sensitive areas are located within regions activated during mental rotation and not in areas activated during saccades.

We were also interested in evaluating whether prefrontal regions implicated previously in object model verification would be activated during mental rotation and object-decision. While the MVPT variant is agnostic about prefrontal activity, the more general, model verification theory, from which it is derived, predicts that ventrolateral prefrontal cortex (VLPFC) areas implicated in working memory, attention and cognitive control should be activated during object cognition (Ganis et al., 2007). In line with this prediction, mental rotation and object-decision activated the VLPFC.

## Methods

The mental rotation task was followed by the object-decision task, or vice versa, counterbalanced across participants. The saccade task was last. Standard blocked designs were used to maximize activation and signal to noise ratio. The tasks were administered on a MacIntosh G3 Powerbook computer. Stimuli were projected via a magnetically shielded video projector onto a translucent screen placed behind the head of each subject. A front-surface mirror mounted on the head coil allowed participants to view the screen. Before neuroimaging, health history and Edinburgh Handedness (Oldfield, 1971) questionnaires were administered.

### Object-decision task

#### Materials

Two image conditions used in standard fMRI localizers for posterior object-sensitive areas were employed (Fig. 1A): 1. *Intact Objects* used photographs of real objects, and 2. *Scrambled* used images of the same objects but with the phases of the spatial frequencies scrambled completely to yield an unidentifiable texture-like image (Malach et al., 1995). Object categories included animals, furniture, vehicles, fruits and vegetables, musical instruments, and tools. *Fixation* images had a black dot at the center on a background that was the mean luminance of the experimental pictures. Since object view may affect results, based on MVPT we obtained ratings of goodness of view from 5 independent raters who rated how good the view of each object was on a 7-point Likert scale: (1) worst view, (2) very poor view, (3) poor view, (4) moderate view (neither poor nor good), (5) good view, (6) very good view, (7) best view. Results indicated that the views were good on average ( $\mu=5.9$ ,  $SD=0.3$ ).

#### Design and procedure

Using *PsyScope* software (Cohen et al., 1993), six blocks each of *Intact* and *Scrambled* conditions alternated. The run started with either *Intact* or *Scrambled*, counterbalanced across participants. Blocks of *Intact Objects* (e.g., animals) and their corresponding *Scrambled* version (e.g., scrambled animals) were shown consecutively since each scrambled set was the control for its corresponding intact object category. Order of the six types of category blocks (animal, furniture, vehicle, fruit–vegetable, Tools-A, Tools-B with musical instruments) was counterbalanced across participants in a Latin square design. Each block had 16 trials. On each trial, a picture was shown for 1875 ms followed by 125 ms of the *Fixation* image. For each picture, participants performed an object categorization task, pressing one button as soon as they could categorize the object or another button if the image was a scrambled ‘non-sense’ picture. The run started and ended with 20 s of fixation. Before the run, participants received instructions and practiced the task with non-experimental images.

### Mental rotation task

#### Materials

For mental rotation images (Fig. 1B), line drawings with pairs of four types of Shepard–Metzler cube objects (rotated in 20° in-depth rotation increments from 20° to 180°) were taken from our prior work (for details, see Amick et al., 2006). From these, 144 no rotation (0°) control pictures were constructed, as in prior

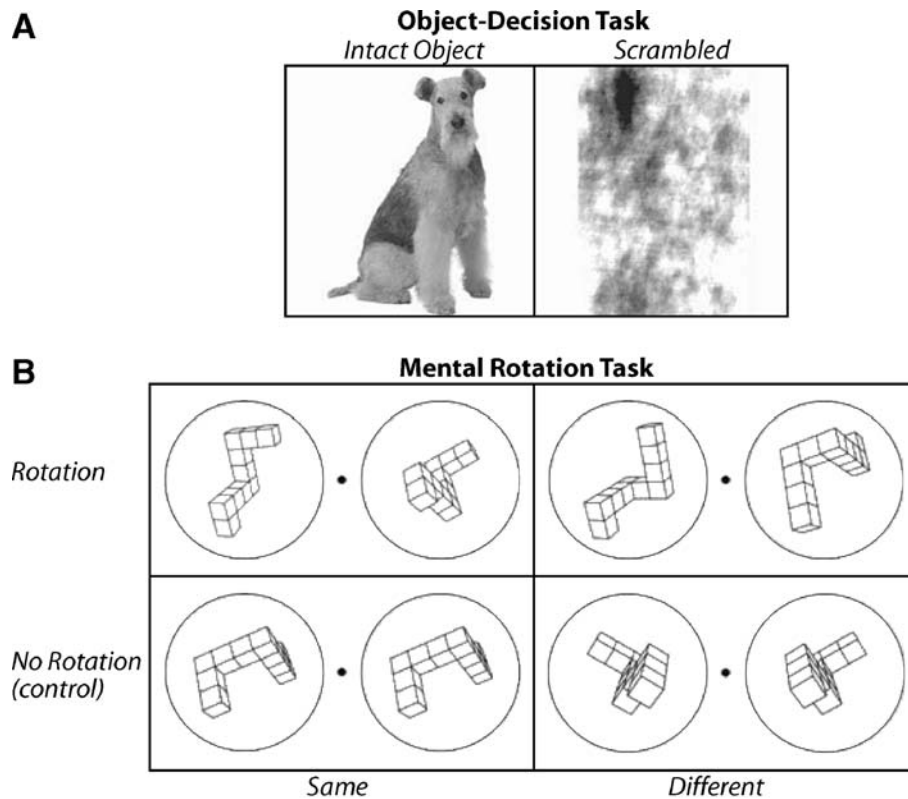


Fig. 1. (A) Object-decision task. Intact pictures of real objects and phase scrambled versions of the same objects alternated in separate blocks. Participants pressed one key as soon as they categorized the *Intact Object* (e.g., as a dog; sample picture at left) or realized the image was a non-sense figure (i.e., *Scrambled*; sample picture at right). (B) Mental rotation task. Participants fixated a central dot and decided whether the object on the right side was exactly the same as or different from (i.e., the mirror image of) the object on the left. Each panel shows one of the four types of three-dimensional (3D) objects in the experiment. All rotations were in-depth along a  $y$ -axis. For the Rotation condition, angular disparity was  $20^{\circ}$ – $180^{\circ}$  between the two objects. Rotation examples show *Same* objects rotated  $60^{\circ}$  from each other and *Different* objects (mirror images) rotated  $140^{\circ}$  from each other. For the No Rotation control condition ( $0^{\circ}$  angular disparity between the two objects), examples show two pictures of the Same object, both at  $120^{\circ}$  from the target  $0^{\circ}$  angle used in the Rotation conditions, and Different objects are mirror images, both at  $100^{\circ}$  from the target  $0^{\circ}$  angle used in the Rotation conditions.

neuroimaging studies (Cohen et al., 1996; Kosslyn et al., 1998). The entire image, including circles, subtended about  $5^{\circ}$  of visual angle vertically and a little over  $11^{\circ}$  horizontally so that the widest angle subtended by any rotated object pair would be within  $11^{\circ}$ , the size of objects in the object-decision task.

#### Design and procedure

We used the standard mental rotation task (Fig. 1B) from prior work (Cohen et al., 1996; Kosslyn et al., 1998). Using *PsyScope* software (Cohen et al., 1993), in one run, 6 blocks of the mental *Rotation* condition alternated with 6 blocks of the no rotation *Control* condition; note, one subject did 4 and another 7 blocks. The run started with either mental rotation or the control condition, counterbalanced across participants. Each block lasted 30 s with an inter-block interval of one TR (2 s) and up to 24 unique object pairs. Each object pair was shown until response (Seurinck et al., 2005), and the fixation stimulus, consisting of the fixation dot and two circles but no objects, was then shown for 500 ms before the next object pair. The run began and ended with 20 s of the fixation stimulus. Before the mental rotation run (and during the second anatomical scan), participants received detailed task instructions and extensive practice using a non-experimental object ( $20^{\circ}$  increments from  $10^{\circ}$  to  $170^{\circ}$ ). Each of the four types of

experimental objects was then shown until the subject pressed a key to go on, and twice each to minimize stimulus repetition effects during the mental rotation experiment run.

#### Saccade task

##### Materials

Using *PictPresenter* software, in the *Saccade* condition, a white dot on a black background appeared for 30 ms centered on the screen and then moved randomly to one of four horizontal locations ( $5$  or  $10^{\circ}$  to the right or left visual field) or back to center at an inter-trial interval of 500 ms. In the *Fixation* condition, the dot remained centered.

##### Design and procedure

The activation paradigm was adapted from Petit et al. (1997). In one scanning run, four blocks each of the saccade and fixation conditions alternated. Each block lasted 20 s, and the starting condition was counterbalanced across participants; runs ending with a moving dot had an extra 20 s of fixation. Participants moved their eyes to each location in the saccade condition and fixated the dot in the fixation condition, receiving instructions and practice just before the scanning run.

### MRI data acquisition

High-resolution T1-weighted scans (MP-RAGE; FOV=256 mm×256 mm, matrix 192×256, TR=6.6 ms, TI=300 ms, TE=2.9 ms, flip=8°, thickness=1.33 mm) for anatomical localization and T2\*-weighted, blood oxygenation level dependent (BOLD), functional scans were acquired at 3 T (*Siemens Allegra*) with a whole-head coil. Before the first functional scan, a T1-weighted echo-planar image (EPI) image was acquired for later co-registration of anatomical with functional images. Functional imaging used a gradient-echo EPI pulse sequence to acquire 21 AC–PC slices (5 mm thick; 1 mm skip; TR=2 s, TE=30 ms; flip angle=90°, 64×64, 3×3 mm voxels). A second MP-RAGE scan was usually acquired during practice for the mental rotation task.

### MRI data analyses

Using SPM99 software (Wellcome Department of Cognitive Neurology), anatomical scans were co-registered with the functional scans using the T1-EPI image. The co-registered anatomical images were then normalized to Montreal Neurological Institute (MNI305) stereotactic space (interpolating to 3-mm<sup>3</sup> voxels; neurological convention). Pre-processing of fMRI BOLD data included motion correction, normalization, and spatial smoothing (8-mm<sup>3</sup> Gaussian kernel). For normalization, the parameters from the anatomical images were used to ensure optimal registration of structural and functional images. Statistical analyses used the general linear model. High-pass filtering was applied, but global signal scaling was not used to avoid spurious deactivations. Design matrices were modeled using a boxcar function convolved with a canonical hemodynamic response function. Motion regressors were included as variables of no interest in the design matrices for saccade and object-decision data. Activation was assessed in linear contrasts between two conditions for each task. Contrast images for each subject were used in second-level analyses treating subjects as a random effect. One-sample *t*-tests assessed contrasts. Results were evaluated using standard thresholds of uncorrected  $p_u < 0.001$  since our regions of interest were those reported in prior work, but, for a more stringent analysis to reveal any additional regions of interest, we also used the false discovery rate (FDR) correction for multiple voxel-wise comparisons across the whole-head at  $p_{FDR} < 0.05$ , balancing type I and II errors (Genovese et al., 2002). To define regions of interest (ROIs) based on published coordinates, an automated algorithm extracted clusters of activation (16 mm radius) from each of the group averaged, random effects contrasts of saccade, mental rotation, and object-decision results, separately (Worsley et al., 1996). ROI clusters that overlap with the published coordinates of regions implicated in saccade, mental rotation, and object-sensitive activity were defined as the published functional area, applying the tal2mni conversion utility, as needed, to map published Talairach (Talairach and Tournoux, 1988) and MNI305 coordinates. Two VLPFC ROIs were based on published coordinates for object model verification and visual memory effects (Ganis et al., 2007; Kirshhoff et al., 2000): anterior VLPFC (aVLPFC; BA 45/47/12; ±37 26 5) and posterior VLPFC (pVLPFC; BA 44/6; ±48 9 34). The defined ROI clusters were used to more precisely define the regions activated during mental rotation (Supplementary Fig. 5A) and object-decision (Supplementary Fig. 5B) and their overlap. Brain structures were labeled based on a human brain atlas

(Duvernoy et al., 1999). To determine the location of overlapping voxels, the SPMs for object-decision and mental rotation tasks, as well as the saccade task SPM, were overlaid on the same MNI305 individual canonical brain.

### Participants

Twenty young, neurologically normal people volunteered; data sets from two participants were unusable due to scanner malfunction; two others did not complete any tasks. Data were analyzed from 16 participants for the object-decision task ( $M=21.2$  years old; 15.0 years education; 9 females), 13 for the mental rotation task ( $M=21.6$  years old; 15.3 years education; 7 females), and 12 for the saccade task ( $M=21.9$  years old;

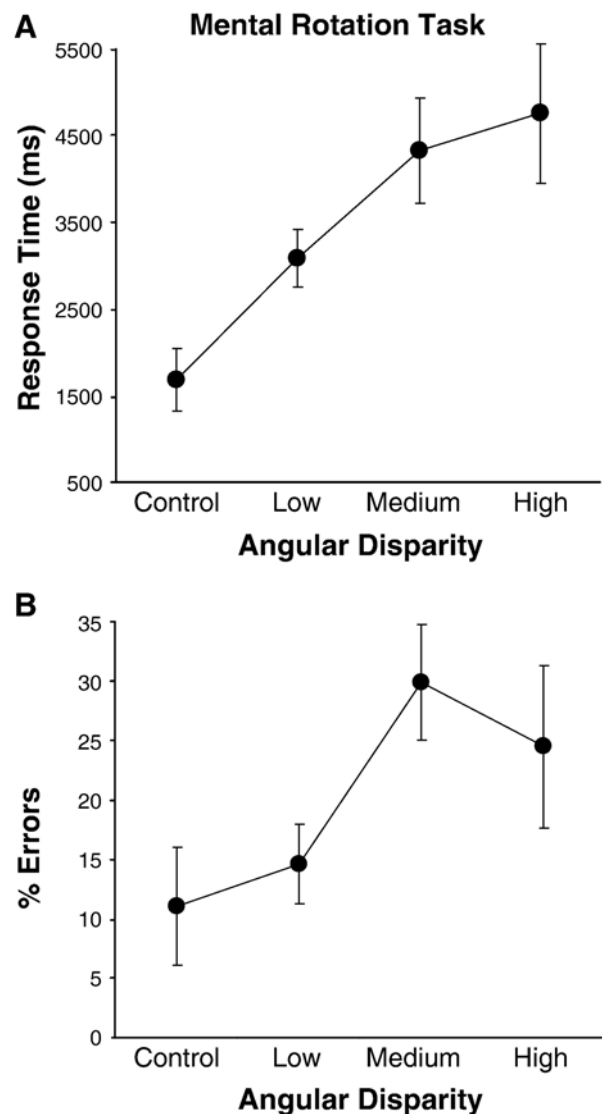


Fig. 2. Performance on the mental rotation of objects task. RTs and accuracy on control (0° or no rotation) blocks were compared to the mental rotation blocks for which the nine rotation angles were collapsed into three levels of depth rotation: low (20°, 40°, 60°), medium (80°, 100°, 120°), and high (140°, 160°). (A) Mean response times showed the typical linear increase with higher rotation angles. (B) Mean percent errors showed the typical linear increase with higher rotation angles.

Table 1

Saccade task (*Saccade*>*Fixation*): Z-scores of most significantly activated volume cluster (>8 mm apart) for each region

Region	Z	MNI coordinate (mm)		
		x	y	z
<b>Frontal</b>				
Frontal eye fields	3.83	-42	-12	54
Frontal eye fields	4.08	48	0	54
<b>Parietal</b>				
aIPS	3.91	30	-54	51
pIPS	3.70	-18	-78	48
iIPS	3.49	-27	-72	24
<b>Occipital</b>				
Cuneus; calcarine sulcus	3.84	-15	-93	0
Cuneus; retrocalcarine sulcus	3.94	21	-93	12
Middle occipital gyrus (O2), superior part	3.75	-30	-78	3
Inferior occipital gyrus (O3)	3.62	-39	-78	-12
Inferior lingual gyrus (O5)	4.23	-21	-57	-15
Anterior calcarine sulcus	3.37	18	-48	0
<b>Other</b>				
Brainstem	4.10	9	-30	-24
Cerebellum	3.99	6	-81	-36
Thalamus (lateral geniculate)	3.32	-21	-24	-6

Note. All uncorrected  $p < 0.001$ . MNI=Montreal Neurological Institute. Brain structures labeled based on Duvernoy et al. (1999). Frontal eye fields at precentral sulcus and posterior tip of superior frontal sulcus; aIPS=anterior part of superior intraparietal sulcus; pIPS=posterior part of superior intraparietal sulcus; iIPS=inferior intraparietal sulcus.

15.5 years education; 6 females). All were right-hand dominant, except one who was left-handed (Oldfield, 1971).

## Results

### Performance

#### Object-decision task

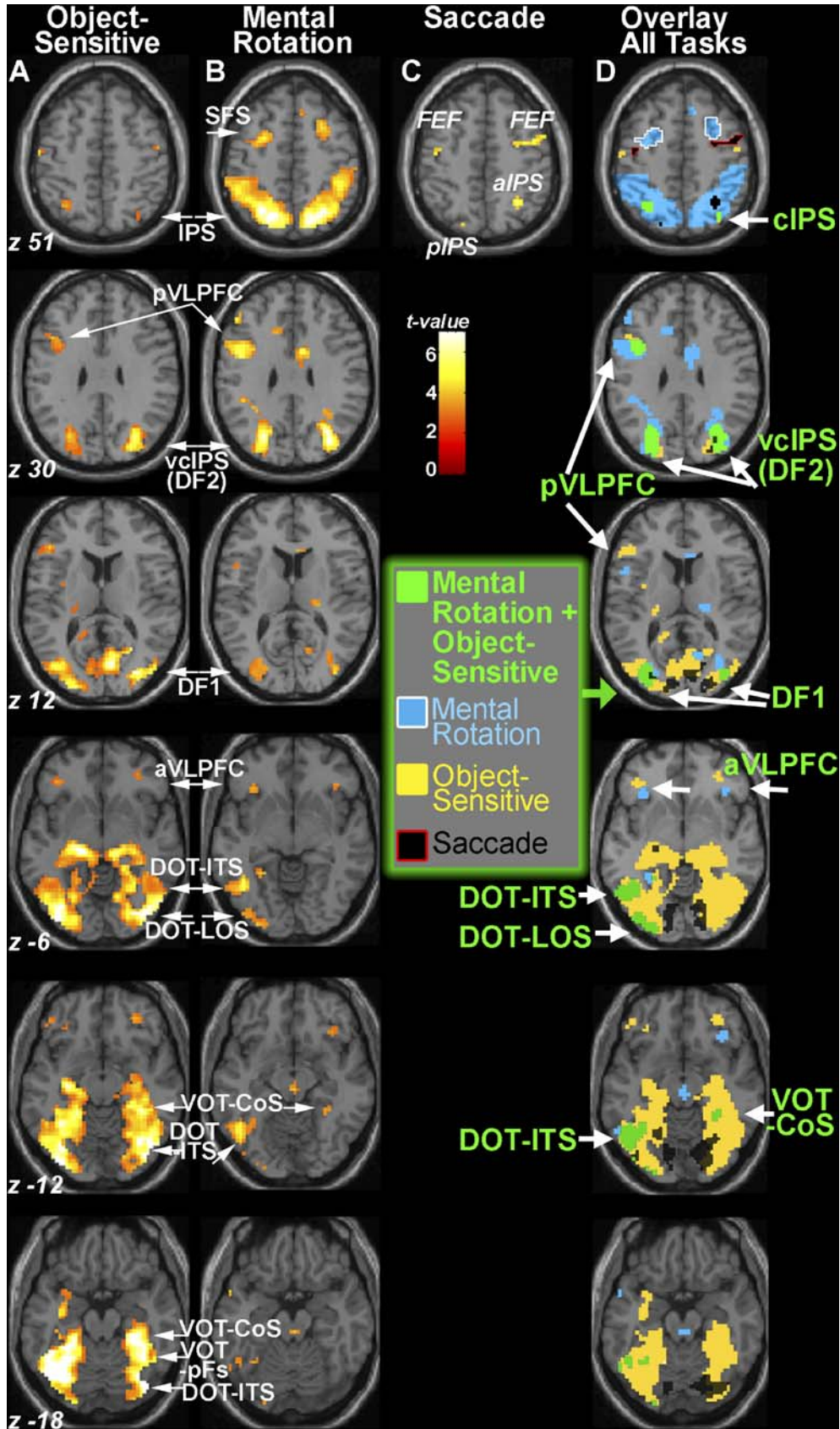
Object-decision accuracy was the same (99.9%) on average in both *Intact* and *Scrambled* conditions.

#### Mental rotation task

Nine rotation angles were collapsed into three levels of rotation: low (20°, 40°, 60°), medium (80°, 100°, 120°), and high (140°, 160°, 180°), as in our prior work (Amick et al., 2006). For response times (RTs), to remove outliers, a cut-off of the mean  $\pm$  2.5 SDs was applied to each of the three rotation levels and the control condition, separately. RT and accuracy measures were subjected to repeated measures ANOVAs with an angular disparity factor (no, low, medium, and high). The characteristic increase in RT with higher angular disparity was significant,  $F(3,36)=12.94$ ,  $p < 0.001$ ,  $\epsilon=0.563$ ; Huynh–Feldt adjustment to degrees of freedom corrected for violation of the sphericity assumption. A planned linear contrast demonstrated that the typical linear mental rotation curve was obtained,  $F(1,12)=16.16$ ,  $p=0.002$ . Planned pairwise comparisons (Bonferroni alpha 0.0125) showed further that RT increased significantly with rotation angle, that is, for control ( $\mu=1684$  ms) versus low ( $\mu=3088$  ms;  $p < 0.001$ ), and low versus medium ( $\mu=4333$  ms;  $p=0.019$ ), though medium versus high did not differ ( $\mu=4541$  ms;  $p > 0.6$ ). The characteristic decrease in accuracy with higher angular disparity was also significant,  $F(3,36)=7.44$ ,  $p=0.001$ . Accuracy was 89% for the control condition, and 85% for low, 70% for medium, and 75% for high mental rotation. A planned linear contrast demonstrated that the typical linear mental rotation curve was obtained,  $F(1,12)=11.20$ ,  $p=0.006$ . Planned pairwise comparisons showed significant differences between only low and medium ( $p=0.001$ ); note that, for post hoc comparisons, control differed from medium ( $p=0.004$ ) and high ( $p=0.017$ ), and low differed from high ( $p=0.049$ ). Since the fMRI results reflect all trials, we emphasize these performance results.

However, performance data were re-analyzed without the 180° condition, which sometimes differs from other high depth rotations (Metzler and Shepard, 1982): 140° and 160° rotations for the high level (RT  $\mu=4759$  ms; accuracy  $\mu=76\%$ ). Results were similar to when the high condition included 180°. Angular disparity was significant for RTs,  $F(3,36)=13.65$ ,  $p < 0.001$ ,  $\epsilon=0.569$ , and for accuracy,  $F(3,36)=5.58$ ,  $p=0.003$ . The planned contrast testing for a linear mental rotation curve was significant for RTs (Fig. 2A),  $F(1,12)=18.05$ ,  $p=0.001$ , and for

Fig. 3. fMRI results for object-decision, mental rotation, and saccade tasks, separately, (scale shows  $t$ -values), and overlaid on each other, all of which are superimposed on axial slices of an individual canonical anatomical MNI brain. Left side of each slice is left hemisphere. For labeled regions of interest, see also Supplementary Fig. 5. (A) Object-decision task activation (*Intact*>*Scrambled*;  $p_{FDR} < 0.05$ ) shows object-sensitive regions in two dorsal occipitotemporal areas (DOT) around the lateral occipital sulcus (DOT-LOS) and the inferior temporal sulcus (DOT-ITS), two ventral occipitotemporal areas (VOT) around the medial bank of the fusiform gyrus (VOT-pFs; see  $z = -12$  and  $-18$ ) and the collateral sulcus (VOT-CoS; see  $z = -12$  and  $-18$ ), and two dorsal foci, DF1 around the transverse occipital sulcus and DF2 in ventral-caudal IPS (vcIPS). Activation was also found in ventrolateral prefrontal cortex (VLPFC) in a left posterior region (pVLPFC; see  $z = 30$ ) and a bilateral anterior region (aVLPFC BA 45 and part of BA 47; see  $z = -6$ ). (B) Mental rotation activation (*Rotation*>*Control*;  $p_{FDR} < 0.05$ ) was found in left pVLPFC, bilateral aVLPFC (BA 47/12), anterior cingulate, and bilateral superior frontal sulcus SFS [BA 8]; see  $z = 51$  in the frontal lobe, and a swath of posterior occipitoparietal regions in and around the intraparietal sulcus (IPS) bilaterally in DF1, vcIPS (DF2), and caudal IPS (cIPS; around retinotopic area IPS2), and more superior and anterior parietal regions. (C) Saccade-related activation (*Saccade*>*Fixation* at  $p_u < 0.001$ ) was found anteriorly in bilateral frontal eye fields (FEF) overlapping the precentral sulcus ( $-42 -12 54$ ;  $48 0 54$ ) and right posterior tip of the superior frontal sulcus (BA 6;  $36 -3 51$ ). Activation was also found in posterior eye fields in the intraparietal sulcus (IPS) in a left posterior (pIPS;  $-18 -78 48$ ) and a right anterior IPS region (aIPS;  $30 -54 51$ ). (D) The SPM for mental rotation and the SPM for saccades overlaid on the SPM for object-decision. Regions of overlap between object-decision and mental rotation (but not saccade) tasks are shown in green, and green text and white arrows label them. Saccade task activation (*Saccade*>*Fixation* at  $p_u < 0.001$ ; black) is shown in the frontal eye fields (FEF; black with red stroke at  $z = 51$ ) and the pIPS and aIPS. Mental rotation task activation (*Rotation*>*Control* at  $p_{FDR} < 0.05$ ; blue) included saccade areas in the pIPS and aIPS but not FEF. Regions outside saccade areas were also activated: posterior part of the superior frontal sulcus (blue with white stroke at  $z = 51$ ) and more caudal areas of posterior cortex in occipital, parietal, and temporal cortex, which are regions that overlapped object-sensitive areas. Object-decision task activation (*Intact*>*Scrambled*;  $p_{FDR} < 0.05$ ; yellow) defined object-sensitive areas. Regions of overlap between object-decision and mental rotation activation (green), which did not overlap with saccade activity, areas. Regions of overlap between object-decision and mental rotation activation (green), which did not overlap with saccade activity, areas. Regions of overlap between object-decision and mental rotation activation (green), which did not overlap with saccade activity, were found in ventral caudal intraparietal sulcus (vcIPS/DF2 at  $z = 30$ , which appeared to overlap with retinotopic area IPS1 extending caudally into V7) and occipital area DF1 ( $z = 12$ ; this appeared to overlap with retinotopic areas V3AB-V7). Mental rotation activation was also found to overlap with object-sensitive areas of bilateral VOT-CoS and left DOT-ITS and DOT-LOS. Other object-sensitive areas of VOT-pFs, mid parts of left DOT, and right DOT were not activated during mental rotation.



accuracy (Fig. 2B),  $F(1,12)=11.36$ ,  $p=0.006$ . The planned pairwise comparison did not show a difference between medium and this high condition for both RTs and accuracy ( $ps>0.3$ ).

## fMRI

### Saccade task

Frontoparietal regions previously implicated in saccadic eye movements (Astafiev et al., 2003) were successfully defined using data from the saccade task. For the contrast of *Saccade>Fixation* (Table 1, Figs. 3C–D), activation was found at  $p_u<0.001$  (note, none at  $p_{FDR}<0.05$ ) in frontal eye fields (FEF), a region encompassing precentral sulcus and the posterior tip of the superior frontal sulcus, and intraparietal sulcus (IPS) areas in the anterior IPS (aIPS) and posterior IPS (pIPS) (Astafiev et al., 2003), as well as some retinotopic areas in occipital cortex (possibly V1, V2v, V2d, V3v, V3d, V3A, V4, V7) (Brewer et al., 2005; Silver et al., 2005), extending into the most inferior part of the IPS at the fundus since the contrast was between multiple retinal locations versus one central location. We explored the opposite contrast of *Fixation>saccade*, finding no significant activation at  $p_{FDR}<0.05$  and activation at  $p_u<0.001$  in the left caudate tail.

For the saccade ROIs, to include the most voxels, a threshold of  $p_u<0.05$  for the saccades>fixation contrast was used for the automated algorithm extracting ROI cluster volumes; we mainly aimed to exclude any saccade-related voxels from the other task results, and so wanted to be sure to capture even weak saccade activity. Bilateral FEF and aIPS and pIPS clusters were selected based on the MNI coordinates of published saccade cue and target areas (Astafiev et al., 2003). These clusters were combined into one VOI mask and used to exclude saccade-related voxels from all mental rotation and object-decision task results by applying the SPM exclusive masking procedure.

### Object-decision task

Using the contrast of *Intact>Scrambled* (Table 2; Fig. 3A and Supplementary Fig. 5A), activation during the object-decision task was found at  $p_{FDR}<0.05$  (i.e., false discovery rate (FDR), whole-head correction) (Genovese et al., 2002) in the six posterior ROIs defined previously as object-sensitive areas (Grill-Spector et al., 2000; Hasson et al., 2003): two dorsal occipitotemporal areas (DOT) around the lateral occipital sulcus (DOT-LOS) and the occipitotemporal sulcus and inferior temporal sulcus (DOT-ITS), two ventral occipitotemporal areas (VOT) around the medial bank of the fusiform gyrus (VOT-pFs) and the building-selective area in the collateral sulcus (VOT-CoS), and two dorsal foci: the DF1 extended from the transverse occipital sulcus (DOT-TOS), a region which shows selectivity for buildings (Grill-Spector and Malach, 2004; Hasson et al., 2003), dorsally through middle occipital gyrus and into the intraoccipital sulcus. The DF1 location was around retinotopic areas V3AB perhaps extending superiorly into area V7, though DF1 extended more laterally than V7 is found (Silver et al., 2005; Tootell et al., 1998). The DF2 is at the most ventral-caudal IPS region (vcIPS) and lies just superior, anterior, and medial relative to DF1 (Aguirre et al., 1998; Epstein et al., 1999; Grill-Spector et al., 2001; Grill-Spector and Malach, 2004) and seemed to extend inferiorly into retinotopic area V7 (Silver et al., 2005).

The DF2 is around the location of retinotopic area IPS1, though DF2 tends to extend more laterally (Silver et al., 2005); we will henceforth refer to DF2 by the anatomical label of vcIPS. In the medial temporal lobe, the posterior head and especially body and tail of the hippocampus were also activated (Supplementary Fig. 6). In the frontal lobe, activation was found in bilateral anterior ventrolateral prefrontal cortex (aVLPFC) and left posterior VLPFC (pVLPFC) areas of inferior precentral and frontal sulci, as well as premotor and motor cortex and orbital and insular cortex. At  $p_u<0.001$ , the same posterior regions were activated but none in VLPFC. At both thresholds, the same regions were activated with or without saccade voxels exclusively masked out. We explored the opposite contrast of *Scrambled>Intact*, finding activation at  $p_u<0.001$  in right angular gyrus, a part of a ‘default’ state network (e.g., Fox et al., 2005; Vincent et al., 2006); no areas activated at  $p_{FDR}<0.05$ .

### Mental rotation task

For the contrast of *Rotation>Control*, mental rotation-related activation was found in previously reported frontoparietal regions at  $p_{FDR}<0.05$  and  $p_u<0.001$  (Cohen et al., 1996; Jordan et al., 2002; Kosslyn et al., 1998; Podzebenko et al., 2002; Vanrie et al., 2002); as results were similar between thresholds, we focus on those at  $p_{FDR}<0.05$  (Table 3; Fig. 3B and Supplementary Fig. 5B). The mental rotation regions were identified based on the range of bilateral coordinates reported for regions activated consistently in studies of the mental rotation of three-dimensional (3D) cube objects (Barnes et al., 2000; Ecker et al., 2006; Gauthier et al., 2002; Jordan et al., 2002; Kosslyn et al., 1998, 2001; Vanrie et al., 2002) and that show parametric modulation with rotation angle (Podzebenko et al., 2002). In posterior cortex, mental rotation activation was found in the entire bilateral IPS, including the most caudal and ventral part of the IPS (i.e., vcIPS/IPS1), and extending dorsally into superior and inferior parietal gyri (BA 7/39/40), including the caudal IPS (cIPS) region immediately superior to vcIPS/DF2, which appears to correspond to IPS2 (Silver et al., 2005). The dorsal activation extended inferiorly into dorsal occipital cortex, from intraoccipital sulcus into middle occipital gyrus and ending at the most inferior point around the transverse occipital sulcus. This dorsal occipital activation appeared to correspond to retinotopic areas V3AB and V7 (Silver et al., 2005) where we found object-sensitive DF1 activity. Mental rotation activation was also found to extend into the temporal lobe into large parts of the DOT in the left occipitotemporal sulcus and inferotemporal sulcus region (henceforth referred to as DOT-ITS[MR]) and a more posterior dorsal region, more in the left than right hemisphere, in the middle occipital gyrus, extending into the transverse occipital sulcus, around lateral occipital sulcus (henceforth referred to as DOT-LOS[MR]), and a small bilateral part of VOT-CoS. In the frontal lobe, mental rotation activation was found in left pVLPFC and bilateral aVLPFC, anterior cingulate, and a bilateral superior frontal sulcus area (BA 8). While not of interest for our hypotheses, we explored the opposite contrast of *Control>Rotation*. We found activation at  $p_u<0.001$  in bilateral supramarginal gyrus/superior temporal gyrus (−57 −26 22; 68 −38 18) and right precuneus (15 −85 27), and in a small part of left superior temporal sulcus (−60 −47 5) and a small anterior medial part of left superior frontal cortex (−9 60 27), which may be parts of a ‘default’ state network that are anti-correlated with active task networks, such as the frontoparietal networks active during

Table 2  
Object-decision task (*Intact Object*>*Scrambled*): Z-scores of most significantly activated volume cluster (>8 mm apart) for each region ( $p_{FDR}<0.05$ )

Region	Z	$p_{FDR}$	MNI coordinate (mm)		
			x	y	z
<b>Frontal</b>					
Anterior VLPFC (BA 45/47)	3.34	0.009	-45	30	12
Anterior VLPFC (BA 45/47)	3.22	0.011	54	33	21
Posterior VLPFC (BA 44/6)	3.22	0.011	-42	15	30
Inferior precentral sulcus	3.40	0.008	-45	-6	45
Precentral gyrus	3.58	0.005	51	-9	42
Precentral gyrus/central sulcus	3.03	0.017	-24	-21	66
Central sulcus	3.07	0.016	21	-27	66
Lateral orbital gyrus	2.74	0.032	-30	33	-12
Posterior orbital gyrus	3.20	0.012	30	42	-12
Circular insular sulcus	3.09	0.015	-30	-3	15
<b>Parietal</b>					
Intraparietal sulcus	3.00	0.018	33	-63	60
Posterior cingulate sulcus	2.82	0.027	-12	-36	57
<b>Occipital and temporal</b>					
DOT (maximum at DOT-LOS)	6.19	<0.001	-42	-66	-21
VOT (maximum at fusiform gyrus)+MTL	5.95	<0.001	-33	-63	-18
DOT (maximum at DOT-LOS)+VOT+MTL	5.81	<0.001	36	-66	-15
<b>Other</b>					
White matter (anterior cingulate, SFS)	2.85	0.025	18	18	42
Cerebellum	3.18	0.012	-9	-75	-36
Cerebellum	3.73	0.003	6	-60	-39

Note.  $p_{FDR}$ = $p$ -values with false discovery rate (FDR) correction; BA= Brodmann area; MNI=Montreal Neurological Institute. Brain structures labeled based on Duvernoy et al. (1999). VLPFC=ventrolateral prefrontal cortex; anterior VLPFC=VLPFC in inferior frontal gyrus, pars triangularis; posterior VLPFC=VLPFC in inferior frontal sulcus and inferior precentral sulcus; DOT=dorsal occipitotemporal (lateral occipital sulcus [LOS], inferior temporal sulcus); VOT=ventral occipitotemporal (fusiform gyrus, collateral sulcus); MTL=medial temporal lobe structures of the parahippocampal gyrus and hippocampus; SFS=superior frontal sulcus.

working memory and attention (and mental rotation) (e.g., Fox et al., 2005; Vincent et al., 2006); no areas activated at  $p_{FDR}<0.05$ .

#### Comparison between mental rotation, object-decision, and saccade task areas

To assess whether brain regions activated during object-decision, especially object-sensitive DF1 and DF2 (vcIPS), coincide with regions activated during mental rotation but not saccades, results were compared across the three tasks. Anatomical overlays of the object-sensitive (*Intact*>*Scrambled*) at  $p_{FDR}<0.05$  and mental rotation (*Rotation*>*Control*) at  $p_{FDR}<0.05$  SPMs and saccade SPMs (*Saccade*>*Fixation*) at  $p_u<0.001$  demonstrated substantial overlap between object-decision and mental rotation tasks but little with saccade-related activity (Figs. 3D and 4). Of the areas defined in the saccade task, the posterior eye fields of the aIPS and pIPS, but not the FEF, were activated during both mental rotation and object-decision, though the activation was bilateral for mental rotation, while the object-decision activations were in the hemisphere opposite that for the saccade task. Among the other areas activated in the saccade task (i.e., outside the eye fields), the small amount of overlap with voxels activated during mental

rotation and especially object-decision probably reflects the retinotopic organization of these visual cortices. After all, both DF1 and vcIPS (approximately V3AB/V7 and IPS1, respectively) are retinotopically organized (Silver et al., 2005), and parts of VOT (VO1 and VO2) and of DOT-LOS (LO1 and LO2) have been shown to have a classic retinotopic organization (Brewer et al., 2005; Larsson and Heeger, 2006). In particular, we observed saccade task activation in a small medial part of right vcIPS that also showed mental rotation and object-decision activity. Small medial parts of DF1 showed bilateral saccade task activation and was object-sensitive bilaterally and, in the left hemisphere, activated during mental rotation. Saccade and object-decision activation overlapped in medial parts of VOT-pFs, perhaps corresponding to retinotopic areas VO1–2, and in the most posterior and medial parts around the DOT-LOS region

Table 3  
Mental rotation task (*Rotation*>*Control*): Z-scores of most significantly activated volume cluster (>8 mm apart) for each region ( $p_{FDR}<0.05$ )

Region	Z	$p_{FDR}$	MNI coordinate (mm)		
			x	y	z
<b>Frontal</b>					
Anterior VLPFC (BA 47/12)	3.28	0.019	-30	24	0
Anterior VLPFC (BA 47/12)	3.31	0.018	36	33	3
Posterior VLPFC (BA 44/6)	3.98	0.010	-45	6	27
DLPFC (BA 9/46)	3.64	0.012	-48	33	27
Superior frontal sulcus (BA 8)	3.89	0.011	-27	3	63
Superior frontal sulcus (BA 8)	3.60	0.013	24	9	57
Medial prefrontal	3.12	0.024	9	36	42
Anterior cingulate gyrus	3.49	0.014	-6	18	24
Anterior cingulate gyrus	3.73	0.011	9	6	30
<b>Parietal</b>					
Superior IPS (BA 7/39/40)	4.48	0.010	-24	-66	60
Ventral caudal IPS (DF2)+DF1	4.54	0.010	33	-75	30
<b>Occipital</b>					
DF1+DOT-LOS	4.55	0.010	-36	-78	18
<b>Temporal</b>					
DOT-ITS	3.96	0.010	-39	-54	-3
DOT-ITS+VOT-fusiform gyrus	3.20	0.021	-33	-54	-15
VOT-collateral sulcus	3.20	0.021	-27	-48	-6
VOT-collateral sulcus	3.39	0.016	30	-42	-9
Superior temporal sulcus	3.37	0.017	-42	-33	3
Superior temporal gyrus	3.25	0.020	-54	9	-18
<b>Other</b>					
Lateral posterior thalamus or pulvinar	3.57	0.013	24	-21	6
Caudate tail	3.26	0.019	-33	-30	3
Globus pallidus	2.97	0.030	18	0	3
Brainstem	3.21	0.021	3	-24	-12
Brainstem	2.90	0.033	0	-33	-33
Cerebellum	3.99	0.010	6	-81	-33
Cerebellum	3.83	0.011	30	-72	-33
Cerebellum	2.88	0.035	6	-63	-39

Note.  $p_{FDR}$ = $p$ -values with false discovery rate (FDR) correction. MNI=Montreal Neurological Institute. BA=Brodmann area. Brain structures labeled based on Duvernoy et al. (1999). VLPFC=ventrolateral prefrontal cortex; anterior VLPFC=VLPFC in horizontal ramus of the lateral fissure; posterior VLPFC=VLPFC in inferior frontal sulcus and inferior precentral sulcus; DLPFC=dorsolateral prefrontal cortex; IPS=intraparietal sulcus; DF=dorsal foci where DF1 corresponds to V3AB/V7; DOT=dorsal occipitotemporal; DOT-LOS=DOT-lateral occipital sulcus; DOT-ITS=DOT-inferior temporal sulcus; VOT=ventral occipitotemporal.

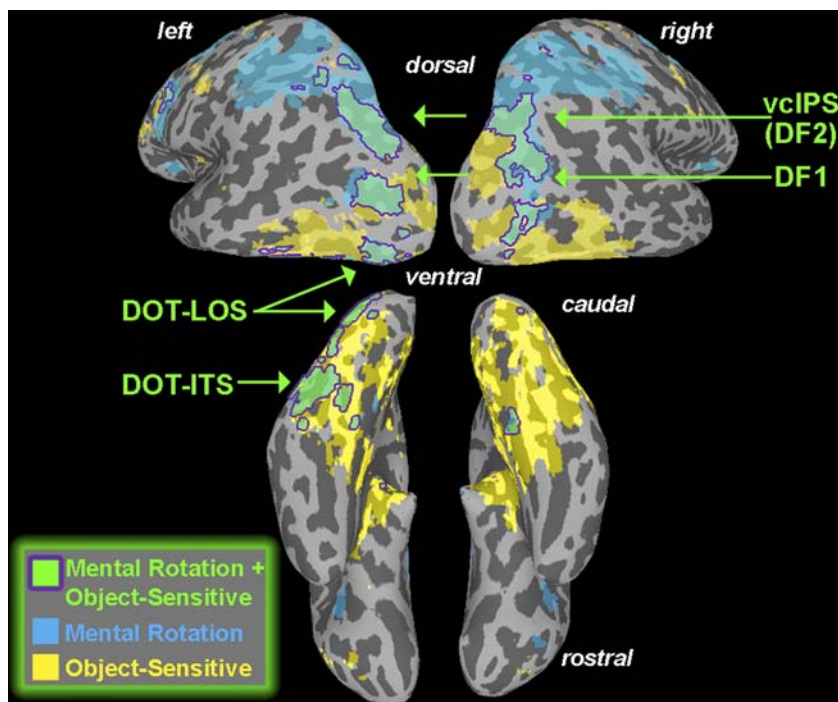


Fig. 4. Overlay of activation maps during object-decision and mental rotation tasks on posterior views (top) and ventral views (bottom) of an average inflated brain, which were created with FreeSurfer (Dale et al., 1999; Fischl et al., 1999) from 27 anatomical scans obtained from MNI and UCLA (Holmes et al., 1998) to better reveal activity within sulci. SPM for mental rotation (blue at threshold of  $t=3.10$ , corresponding approximately to  $p_{FDR}<0.05$ ) overlaid on the SPM for object-decision (yellow;  $t=2.85$ , corresponding approximately to  $p_{FDR}<0.05$ , except that the aVLPFC activation evident in Fig. 3 is below this  $t$ -value). Regions where these areas overlap in vcIPS (DF2), DF1, DOT-ITS, and DOT-LOS are shown (green with purple stroke). Right pointing arrows indicate the location of DOT regions. Left pointing arrows indicate the location of DF1 and vcIPS (DF2).

that seemed located in early extrastriate areas V2v, V2d, V3v, V3d, V3A, V4, and V7 but not retinotopic LO1 or LO2 (Brewer et al., 2005; Larsson and Heeger, 2006).

Critically, most of the vcIPS and a central part of DF1 were clearly activated during both object-decision and mental rotation (and not saccades). Notably, however, in vcIPS, object-decision activation extended to more medial parts than activation during mental rotation which extended more anterolaterally, and, in DF1, object-decision activation extended both more medially and laterally than mental rotation, possibly due to the foveal presentation of images in the object-decision task and more lateral location of images for mental rotation (and saccades) or other procedural differences. In most other parts of the IPS, activation was found during mental rotation but not object-decision or saccades: bilateral IPS regions extending anteriorly and/or dorsally into superior and inferior parietal gyri (BA 7/39/40).

Overlap between the two cognitive tasks but not the saccade task was also found in more ventral posterior areas. Regions that were activated during both object-decision and mental rotation but not the saccade task were found in left DOT-ITS, left DOT-LOS, and a small part of the most dorsal section of right DOT-LOS, and a small part of VOT-CoS bilaterally. Mental rotation activation in the DOT-ITS[MR] subregion was located in an anterior part of the DOT-ITS region activated during object-decision at the border of the anterior occipital and inferior temporal sulci, extending a few voxels into fusiform gyrus. Furthermore, mental rotation activation in the DOT-LOS[MR] in the middle occipital gyrus overlapped the DOT-LOS region

activated during object-decision, extending into the transverse occipital sulcus and located ventral, posterior, and medial to MT+/V5. While overlap with MT+ cannot be ruled out, the DOT[MR] subregions lie ventral to MT+, as defined by anatomical landmarks (Dumoulin et al., 2000; Huk et al., 2002) and functional coordinates (Morone et al., 2000), and DOT-ITS[MR] is anterior and DOT-LOS[MR] is posterior to MT+.

In the frontal lobe, activation for mental rotation but not object-decision was found in anterior cingulate and a bilateral superior frontal sulcus region (BA 8), lying just anterior to the FEF, which was evident only in the saccade task. Both mental rotation and object-decision but not the saccade task activated the same region of left pVLPFC (BA 44/6). However, the bilateral aVLPFC activation during mental rotation was more posterior and located more in the deep part of the horizontal and vertical ramus of the lateral fissure (BA 47/12) than that during object-decision, for which the activation was located more laterally on the inferior frontal gyrus, pars orbitalis and pars triangularis (BA 45), extending slightly into lateral orbital gyrus (part of BA 47/12). We thus evaluated whether overlap would be found with a liberal threshold of  $p_u<0.05$  to reveal the entire activated region. While some overlap in aVLPFC was found bilaterally, especially in the left hemisphere, the activated regions were still largely distinct (Supplementary Fig. 7).

## Discussion

Our neuroimaging results provide clear and direct anatomical support for a key prediction of the MVPT variant of object model

verification theories, namely, that regions along the dorsal stream critical for mental rotation can be recruited for visual object cognition (Bülthoff et al., 1995). We found that, during both mental rotation of objects in-depth and a simple object categorization task (and not during a saccade task), the same regions are activated in the ventral caudal IPS (vcIPS) and the occipital region just ventrolateral to it, both of which have been critically implicated in mental rotation (e.g., Corballis, 1997; Ecker et al., 2006; Podzebenko et al., 2002) and correspond, respectively, to the dorsal object-sensitive areas of DF2 and DF1 (e.g., Grill-Spector et al., 2001). In addition, as object model verification theory predicts, in the frontal lobe, VLPFC regions are recruited during both mental rotation and object-decision tasks, implicating a VLPFC–posterior network in spatial and nonspatial tasks and suggesting a general role for this network in visual object cognition. Finally, though not predicted by MVPT, our results reveal that other, more ventral, object-sensitive areas in parts of DOT-ITS and DOT-LOS are also recruited during mental rotation. We note also that the opposite contrasts (control > experimental) for object-decision and mental rotation tasks show activity in the ‘default’ state network typically anti-correlated with an active task network (Fox et al., 2005; Vincent et al., 2006).

*Occipitoparietal, dorsal occipitotemporal, and ventrolateral prefrontal regions activated during both object-decision and mental rotation (and not saccade) tasks*

While dissociations between mental rotation and object categorization tasks have been reported, the results were inconclusive. A case of impaired rotation but spared categorization from unusual orientations (Farah and Hammond, 1988) showed categorization that was ‘normal’ only relative to a control group impaired by brief displays, and accuracy that was still abnormal for upright objects. A case of impaired categorization of unusual views but spared mental rotation (Turnbull and McCarthy, 1996) had occipital damage, and categorization showed a mental rotation curve not seen in the control group, suggesting spared dorsal spatial transformation compensated for impaired ventral processes. Alternatively, mental rotation was not normal since depth rotations were abnormally slow. One prior fMRI study directly compared blocks of mental rotation and short-term recognition of cube objects (Gauthier et al., 2002) and found a similar rotation curve for both mental rotation and recognition in left IPS (−43 −38 53) perhaps anterior to IPS2 (Silver et al., 2005), but object-sensitive areas were not defined, and a categorization task and real objects were not used.

Findings from our three tasks defined brain regions involved in saccadic eye movements, object mental rotation, and object-decision. Activation during the saccade task defined areas previously implicated in saccadic eye movements: the frontal eye fields (FEF) and the posterior eye fields in the anterior parts of superior IPS (pIPS, aIPS), which are analogous to the FEF and areas VIP/LIP in monkey, respectively (Astafiev et al., 2003). This frontoparietal network has been implicated not only in overt attention with saccades but also covert spatial and nonspatial attention, visuomotor computations regardless of effector (e.g., eye, hand), and maintenance of task-relevant representations (Astafiev et al., 2003; Beauchamp et al., 2001; Kanwisher and Wojciulik, 2000). If these functions are the only processes that differ between the experimental and control conditions in the mental rotation and object-decision

tasks, then we should have observed no effects in any region outside of the FEF and superior IPS network. To the contrary, robust effects occurred outside this network.

During object-decision, the activated areas are located in VLPFC, other frontal areas, and the hippocampus, and, most important, in the six posterior object-sensitive areas defined previously (Grill-Spector et al., 2000; Hasson et al., 2003): two dorsal occipitotemporal areas (DOT) around lateral occipital sulcus (DOT-LOS) and inferior temporal sulcus (DOT-ITS), two ventral occipitotemporal areas (VOT) in the fusiform gyrus (VOT-pFs) and collateral sulcus (VOT-CoS), and two dorsal foci, the DF1 and DF2. In the frontal lobe, activation during the object-decision task was found in bilateral anterior VLPFC (aVLPFC; BA 45 and part of BA 47/12) and left posterior VLPFC (pVLPFC; BA 44/6).

During the mental rotation of objects, areas implicated previously in mental rotation were activated, as well as the VOT-CoS (Cohen et al., 1996; Podzebenko et al., 2002; Richter et al., 2000; Vanrie et al., 2002): we found activation in the entire IPS bilaterally, extending into superior and inferior parietal gyri (BA 7/39/40), and in the occipitoparietal and dorsal occipitotemporal cortex lying ventral to the IPS, and, in the frontal lobe, bilateral superior frontal sulcus (BA 8), anterior cingulate, and bilateral aVLPFC (BA 47/12) and pVLPFC.

Our findings from directly overlaying the three tasks demonstrate precisely that the object-sensitive areas of DF1 and DF2 are active during not only the object-decision (i.e., simple object categorization) task but also mental rotation (and minimally or none during saccades). DF2 is at the most ventral and caudal part of the intraparietal sulcus, and so we refer to this region as vcIPS. DF1 is around transverse occipital sulcus (around the location of retinotopic areas V3AB-V7) lying just ventrolateral to the vcIPS and dorsal to DOT-LOS. vcIPS is located within the region referred to variously in prior mental rotation neuroimaging studies as inferior parietal cortex, angular gyrus, superior parietal lobule, and/or BA 19, and DF1 corresponds to the ventral portion of this region (Barnes et al., 2000; Carpenter et al., 1999; Cohen et al., 1996; Jordan et al., 2002; Richter et al., 2000). vcIPS and DF1 are within the critical regions for mental rotation, being responsible for the characteristic scaling of performance with angular disparity (Barnes et al., 2000; Carpenter et al., 1999; Cohen et al., 1996; Corballis, 1997; Harris et al., 2000; Jordan et al., 2002; Podzebenko et al., 2002; Richter et al., 2000; Vanrie et al., 2002). In addition, we found that a region near retinotopic area IPS2 ( $z$  51) (Silver et al., 2005), located immediately dorsal to vcIPS, includes the saccade-related areas of the aIPS and pIPS (Astafiev et al., 2003) but had previously been included as part of the inferior parietal region critical for scaling of mental rotation performance with angular disparity. Our findings suggest vcIPS (and DF1) would be more appropriate foci for future mental rotation research, instead of the IPS2 region, which may have a role more in saccades and overt attention than spatial rotation.

Activation during mental rotation also includes parts of the more ventral object-sensitive areas in bilateral VOT-CoS and two subregions of the DOT, especially in the left hemisphere. Bilateral VOT-CoS activity has not been reported during mental rotation but has been implicated in processing objects encompassing the peripheral visual field (e.g., buildings), spatial environments, and toy block structures like our cube objects (Epstein et al., 1999; Epstein and Kanwisher, 1998; Hasson et al., 2003). The DOT-ITS [MR] and DOT-LOS [MR] regions have been observed in prior

mental rotation studies but without the monotonic modulation characteristic of the mental rotation process (Just et al., 2001). The DOT-LOS[MR] is near an occipital region reported in prior mental rotation studies (Jordan et al., 2002) and appears to lie within area LO1, one of two retinotopic subregions in object-sensitive DOT-LOS (Larsson and Heeger, 2006). The DOT-ITS[MR] at the border of the anterior occipital and inferior temporal sulci that has been referred to variously as inferior temporal gyrus or motion perception areas of V5/V5A (Barnes et al., 2000; Jordan et al., 2002; Podzebenko et al., 2005; Vanrie et al., 2002). Our findings show that occipitotemporal activity during mental rotation is in object-sensitive DOT regions, which have been found themselves to be motion sensitive (Beauchamp et al., 2002; Hasson et al., 2003; Kourtzi et al., 2002). The results suggest further that the DOT activations are not at the location of MT+ proper, based on anatomical landmarks (Dumoulin et al., 2000; Huk et al., 2002) and functional coordinates for MT+ (Morrone et al., 2000), though we cannot rule out that the DOT activation includes part of MT+ since we had no appropriate motion area localizer. As other object mental rotation studies have found a different pattern of laterality, including more bilateral or right hemisphere involvement of DOT-ITS (Jordan et al., 2002; Vanrie et al., 2002), the left laterality of mental rotation activation in DOT-ITS herein probably reflects our instructions to participants to imagine rotating the image in the right visual field (left hemisphere processing) so that it can be matched to the image in the left visual field (Amick et al., 2006); thus, we consider their right hemisphere counterparts also to be regions involved in mental rotation.

In the frontal lobe, object-decision and mental rotation task activation overlap substantially with each other but not with regions of saccade-related activity. Intriguingly, BA 8 was activated only during mental rotation and did not overlap the FEF activation in the saccade task; BA 8 has been implicated in spatial working memory (Courtney et al., 1998) and perceptual decision-making (Heekeren et al., 2004), processes likely to be engaged during mental rotation tasks. More important, both aVLPFC and pVLPFC were activated during mental rotation and object-decision tasks, consistent with the involvement of the inferior prefrontal cortex in both spatial and object working memory (Owen et al., 1998; Stern et al., 2000). Like the occipitoparietal region, the premotor areas of the pVLPFC are considered critical for mental rotation (Richter et al., 2000; Vanrie et al., 2002) and were found herein to show a common region of activation in both mental rotation and object-decision tasks. By contrast, in aVLPFC, a caudomedial part was involved in mental rotation (BA 47/12), while a more rostralateral part was involved in object categorization (BA 45). These findings show that pVLPFC is recruited for both categorization tasks involving matching to long-term memory (i.e., object-decision) and making the perceptual decisions required for short-term structural matching tasks (i.e., mental rotation), whereas there is a functional dissociation between these tasks in the aVLPFC.

#### *Regions activated during object-decision but not during mental rotation (and saccade) tasks: mid-DOT and VOT*

Other ventral posterior areas were activated during object-decision but not during mental rotation: bilateral VOT-pFs, VOT-CoS, and a mid-DOT area ( $\pm 44 - 72 - 6$ ) in between the DOT-ITS [MR] and DOT-LOS[MR] regions, perhaps encompassing the retinotopic part of object-sensitive DOT-LOS in area LO2 (Larsson

and Heeger, 2006). The finding that these more ventral object-sensitive areas were not recruited for mental rotation, except for a small part of object-sensitive VOT-CoS, is consistent with the classic dorsal–ventral, where–what dichotomy (Ungerleider and Haxby, 1994). Contrary to a proposed functional relationship between left pVLPFC and left VOT-pFs for rapid stimulus–response learning (Dobbins et al., 2004; Wig et al., 2005), left pVLPFC was strongly activated during mental rotation but left VOT-pFs was not.

#### *Role of brain regions recruited for mental rotation in visual object cognition*

Altogether, these findings provide clear evidence that parts of object-sensitive areas in dorsal (DF1; DF2/vcIPS) and ventral (DOT-ITS[MR]; DOT-LOS[MR]) posterior cortex, as well as VLPFC regions, that are activated during an object-decision task coincide with the location of regions involved in a mental rotation task (and not a saccade task). While our findings are generally consistent with other theories, such as those explaining attention and working memory phenomena (Courtney, 2004; Kastner and Pinsky, 2004; Postle, 2006), only the MVPT variant of object model verification theory specifically proposes a role for dorsal occipitoparietal regions critical for mental rotation also in visual object cognition (Tarr and Pinker, 1990). Prior work on mental rotation has suggested that both dorsal and ventral posterior systems are modulated as a function of figural complexity and rotation, with inferior parietal and inferior temporal (i.e., DOT-ITS[MR]) areas working together as part of the same top–down prefrontal–posterior network for analyzing, comparing, and matching two shapes during mental rotation tasks, though DOT-LOS[MR] may be primarily visual (Cohen et al., 1996; Koshino et al., 2005).

We propose that the vcIPS and DF1 regions analyze the spatial structure of objects and can, if necessary, transform objects spatially to achieve a task goal, and, in so doing, provide spatial information (e.g., surface, depth) to the ventral stream that is crucial for visual object constancy. The vcIPS and DF1 regions, as well as the DOT area, have been implicated in spatial processing of object structure, each contributing a distinct function. The DOT seems to have a role intermediate between typical ventral “what” and dorsal “where” functions (Hasson et al., 2003), computing the two- and three-dimensional spatial aspects of objects (e.g., stereoscopic structure, symmetry, depth, movement, kinematics), and relations between objects and space (e.g., position, motion, kinematics, scale) required to perform a task (Gilaie-Dotan et al., 2001; Grill-Spector et al., 1999; Hasson et al., 2003; Kourtzi et al., 2002; Moore and Engel, 2001; Sasaki et al., 2005; Van Oostende et al., 1997). Analogously, sections of monkey inferotemporal cortex seem to code object parts in two dimensions with some depth structure from qualitative information about disparity gradient, depth curvature or horizontal disparity (Tanaka, 2003).

The vcIPS and DF1 region has been implicated in perceiving and matching object structure in-depth, spatial cognition and coordinate transformation, stereopsis and symmetry analysis, and grasping objects (Arbib, 2005; Assad, 2003; Beauchamp et al., 2002; Faillelot et al., 2001; Gilaie-Dotan et al., 2001; Kanwisher and Wojciulik, 2000; Milner and Goodale, 1993; Sasaki et al., 2005; Schluppeck et al., 2005; Shikata et al., 2003; Tsao et al., 2003). Analogously, monkey posterior parietal area 7a is involved in constructing the spatial configuration among the parts of objects (Chafee et al., 2005). Bilateral DF1 is in the region

damaged in Balint's syndrome patients who cannot see multiple object shapes simultaneously ("dorsal simultanagnosia"), perceiving only one object shape at a time without discerning its spatial location (Friedman-Hill et al., 1995, 2003; Turnbull et al., 1997b).

Finally, the vcIPS and DF1 regions have been found to be part of a VLPFC–posterior network for an object model verification process that is more strongly recruited to categorize more than less impoverished images of objects, such as degraded pictures or unusual views (Ganis et al., 2007). During model verification, the aVLPFC is thought to control the network interactions, while the dorsal occipitoparietal regions modulate more ventral areas, especially parts of the DOT (Ganis et al., 2007). This predicts that, during visual object cognition, the degree of occipitoparietal recruitment will be a function of stimulus and task requirements for spatial analysis and coordinate system transformation; for example, we showed objects in very good views during a task not requiring a spatial judgment, obtaining a degree of occipitoparietal activity, but more unusual views and a task demanding greater spatial analysis of object structure should recruit occipitoparietal cortex much more than in our object-decision task, as has been found (Altmann et al., 2005; Kosslyn et al., 1994; Noppeney et al., 2006; Sugio et al., 1999).

## Conclusions

It is well-established that the ventral visual pathway supports object analysis and representation, whereas the dorsal pathway supports spatial analysis, but both ventral occipitotemporal and more dorsal areas have been found to be object-sensitive, suggesting a role for the dorsal pathway in object analysis. Our neuroimaging findings clearly support a key prediction of the MVPT variant of object model verification theories: the dorsal object-sensitive areas of vcIPS and DF1, as well as parts of the DOT-ITS and DOT-LOS, are recruited for the mental rotation of objects, a well-established spatial cognition task. Altogether, our findings provide a key link in understanding the role of ventral and dorsal visual areas in visual object perception and mental rotation of objects: regions in occipitoparietal cortex, as well as DOT cortex, have a general role in everyday object cognition, supporting not only mental rotation tasks but also visual object categorization. The function of the occipitoparietal region (vcIPS and DF1) may be to perform the neural computations that are critical for mental rotation, such as the spatial coordinate transformation of images of objects.

## Acknowledgments

Research was supported by grants F32 AG05914 and Tufts University Faculty start-up funds to H.E.S who was also supported by a Faculty Research Award Committee (FRAC) Research Semester Fellowship from Tufts University and NINDS Grant 9R01 NS052914 during preparation of this manuscript. Brain scanning was conducted at and supported by pilot funding to H.E.S. from the MGH/MIT/HMS Athinoula A. Martinos Center for Biomedical Imaging, which is supported by NCRR grant P41RR14075 and the MIND Institute. This study was conducted in the Vision and Memory Neuroimaging Laboratory in the Department of Psychology at Tufts University, and the Vision and Cognition Laboratory in the Department of Psychology, Boston University, and the Cognitive Neuroimaging Laboratory at the

Center for Memory and Brain in the Department of Psychology at Boston University (P50 MH071702). We thank Dr. Giorgio Ganis for helpful comments on an earlier draft of this manuscript and assistance with Fig. 4, Dr. Alice Cronin-Golomb for providing some computer resources for this project, and Dr. David C. Somers and Jascha Swisher for helpful discussion of retinotopic visual areas. We are grateful to Dr. Karin Schon for the saccade task activation paradigm and Courtney Horwitz for assistance with some aspects of the data analyses and scanning.

## Appendix A. Supplementary data

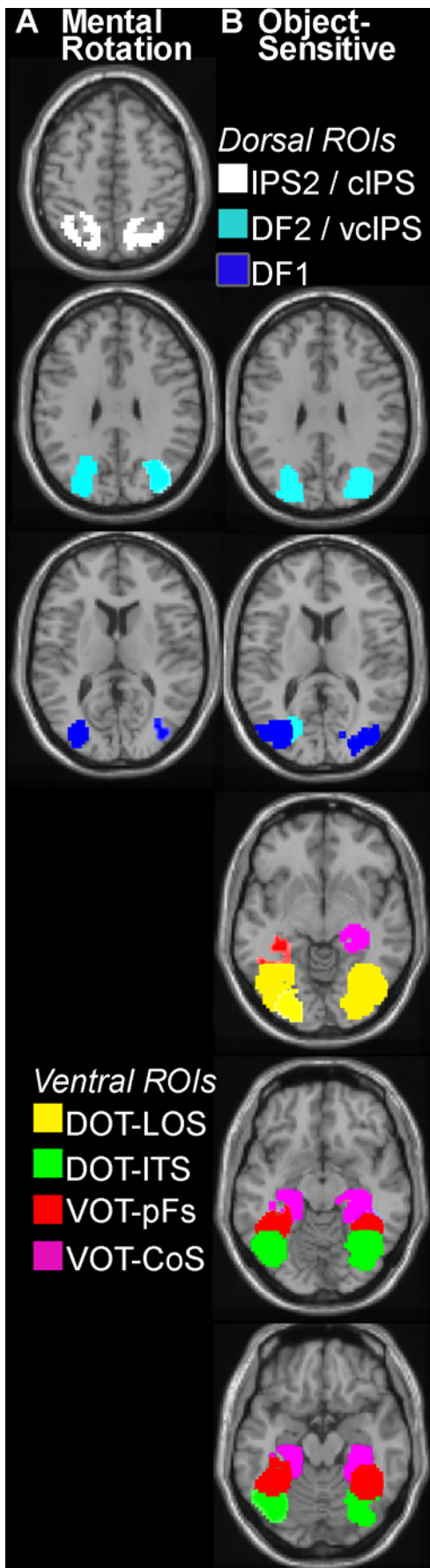
Supplementary data associated with this article can be found, in the online version, at [doi:10.1016/j.neuroimage.2007.01.012](https://doi.org/10.1016/j.neuroimage.2007.01.012).

## References

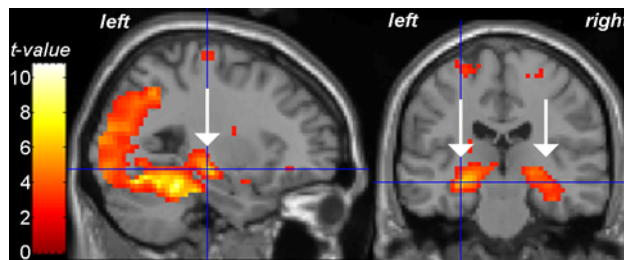
- Aguirre, G.K., Zarahn, E., D'Esposito, M., 1998. An area within human ventral cortex sensitive to "building" stimuli: evidence and implications. *Neuron* 21, 373–383.
- Altmann, C.F., Grodd, W., Kourtzi, Z., Bulthoff, H.H., Karnath, H.O., 2005. Similar cortical correlates underlie visual object identification and orientation judgment. *Neuropsychologia* 43, 2101–2108.
- Amick, M.A., Schendan, H.E., Ganis, G., Cronin-Golomb, A., 2006. Frontostriatal circuits are necessary for visuomotor transformation: mental rotation in Parkinson's disease. *Neuropsychologia* 44, 339–349.
- Arbib, M.A., 2005. From monkey-like action recognition to human language: an evolutionary framework for neurolinguistics. *Behav. Brain Sci.* 28, 105–124 (discussion 125–167).
- Assad, J.A., 2003. Neural coding of behavioral relevance in parietal cortex. *Curr. Opin. Neurobiol.* 13, 194–197.
- Astafiev, S.V., Shulman, G.L., Stanley, C.M., Snyder, A.Z., Van Essen, D. C., Corbetta, M., 2003. Functional organization of human intraparietal and frontal cortex for attending, looking, and pointing. *J. Neurosci.* 23, 4689–4699.
- Barnes, J., Howard, R.J., Senior, C., Brammer, M., Bullmore, E.T., Simmons, A., Woodruff, P., David, A.S., 2000. Cortical activity during rotational and linear transformations. *Neuropsychologia* 38, 1148–1156.
- Beauchamp, M.S., Petit, L., Ellmore, T.M., Ingelholm, J., Haxby, J.V., 2001. A parametric fMRI study of overt and covert shifts of visuospatial attention. *NeuroImage* 14, 310–321.
- Beauchamp, M.S., Lee, K.E., Haxby, J.V., Martin, A., 2002. Parallel visual motion processing streams for manipulable objects and human movements. *Neuron* 34, 149–159.
- Brewer, A.A., Liu, J., Wade, A.R., Wandell, B.A., 2005. Visual field maps and stimulus selectivity in human ventral occipital cortex. *Nat. Neurosci.* 8, 1102–1109.
- Bülthoff, H.H., Edelman, S.Y., Tarr, M.J., 1995. How are three-dimensional objects represented in the brain? *Cereb. Cortex* 5, 247–260.
- Carpenter, P.A., Just, M.A., Keller, T.A., Eddy, W., Thulborn, K., 1999. Graded functional activation in the visuospatial system with the amount of task demand. *J. Cogn. Neurosci.* 11, 9–24.
- Chafee, M.V., Crowe, D.A., Averbeck, B.B., Georgopoulos, A.P., 2005. Neural correlates of spatial judgement during object construction in parietal cortex. *Cereb. Cortex* 15, 1393–1413.
- Cohen, J.D., MacWhinney, B., Flatt, M., Provost, J., 1993. PsyScope: a new graphic interactive environment for designing psychology experiments. *Behav. Res. Methods Instrum. Comput.* 25, 257–271.
- Cohen, M.S., Kosslyn, S.M., Breiter, H.C., DiGirolamo, G.J., Thompson, W.L., Anderson, A.K., Brookheimer, S.Y., Rosen, B.R., Belliveau, J.W., 1996. Changes in cortical activity during mental rotation. A mapping study using functional MRI. *Brain* 119, 89–100.
- Corballis, M.C., 1997. Mental rotation and the right hemisphere. *Brain Lang.* 57, 100–121.

- Courtney, S.M., 2004. Attention and cognitive control as emergent properties of information representation in working memory. *Cogn. Affect Behav. Neurosci.* 4, 501–516.
- Courtney, S.M., Petit, L., Maisog, J.M., Ungerleider, L.G., Haxby, J.V., 1998. An area specialized for spatial working memory in human frontal cortex. *Science* 279, 1347–1351.
- Dale, A.M., Fischl, B., Sereno, M.I., 1999. Cortical surface-based analysis. I. Segmentation and surface reconstruction. *NeuroImage* 9, 179–194.
- Dobbins, I.G., Schnyer, D.M., Verfaellie, M., Schacter, D.L., 2004. Cortical activity reductions during repetition priming can result from rapid response learning. *Nature* 428, 316–319.
- Dumoulin, S.O., Bittar, R.G., Kabani, N.J., Baker Jr., C.L., Le Goualher, G., Bruce Pike, G., Evans, A.C., 2000. A new anatomical landmark for reliable identification of human area V5/MT: a quantitative analysis of sulcal patterning. *Cereb. Cortex* 10, 454–463.
- Duvernoy, H.M., Bourquoin, P., Cabanis, E.A., Cattin, F., 1999. *The Human Brain: Surface, Three-dimensional Sectional Anatomy with MRI, and Blood Supply*, 2nd ed. Springer Verlag, New York.
- Ecker, C., Brammer, M.J., David, A.S., Williams, S.C., 2006. Time-resolved fMRI of mental rotation revisited—Dissociating visual perception from mental rotation in female subjects. *NeuroImage* 32, 432–444.
- Epstein, R., Kanwisher, N., 1998. A cortical representation of the local visual environment. *Nature* 392, 598–601.
- Epstein, R., Harris, A., Stanley, D., Kanwisher, N., 1999. The parahippocampal place area: recognition, navigation, or encoding? *Neuron* 23, 115–125.
- Faillenot, I., Sunaert, S., Van Hecke, P., Orban, G.A., 2001. Orientation discrimination of objects and gratings compared: an fMRI study. *Eur. J. Neurosci.* 13, 585–596.
- Farah, M.J., 1990. *Visual Agnosia: Disorders of Object Recognition and What They Tell Us About Normal Vision*. MIT Press, Cambridge, MA.
- Farah, M.J., Hammond, K.M., 1988. Mental rotation and orientation-invariant object recognition: dissociable processes. *Cognition* 29, 29–46.
- Fischl, B., Sereno, M.I., Dale, A.M., 1999. Cortical surface-based analysis. II: Inflation, flattening, and a surface-based coordinate system. *NeuroImage* 9, 195–207.
- Fox, M.D., Snyder, A.Z., Vincent, J.L., Corbetta, M., Van Essen, D.C., Raichle, M.E., 2005. The human brain is intrinsically organized into dynamic, anticorrelated functional networks. *Proc. Natl. Acad. Sci. U. S. A.* 102, 9673–9678.
- Friedman-Hill, S.R., Robertson, L.C., Treisman, A., 1995. Parietal contributions to visual feature binding: evidence from a patient with bilateral lesions. *Science* 269, 853–855.
- Friedman-Hill, S.R., Robertson, L.C., Desimone, R., Ungerleider, L.G., 2003. Posterior parietal cortex and the filtering of distractors. *Proc. Natl. Acad. Sci. U. S. A.* 100, 4263–4268.
- Ganis, G., Schendan, H.E., Kosslyn, S.M., 2007. Neuroimaging evidence for object model verification theory: role of prefrontal control in visual object categorization. *NeuroImage* 34, 384–398.
- Gauthier, I., Hayward, W.G., Tarr, M.J., Anderson, A.W., Skudlarski, P., Gore, J.C., 2002. BOLD activity during mental rotation and viewpoint-dependent object recognition. *Neuron* 34, 161–171.
- Genovese, C.R., Lazar, N.A., Nichols, T., 2002. Thresholding of statistical maps in functional neuroimaging using the false discovery rate. *NeuroImage* 15, 870–878.
- Gilaie-Dotan, S., Ullman, S., Kushnir, T., Malach, R., 2001. Shape-selective stereo processing in human object-related visual areas. *Hum. Brain Mapp.* 15, 67–79.
- Goodale, M.A., Milner, A.D., 1992. Separate visual pathways for perception and action. *Trends Neurosci.* 15, 20–25.
- Grill-Spector, K., Malach, R., 2004. The human visual cortex. *Annu. Rev. Neurosci.* 27, 649–677.
- Grill-Spector, K., Kushnir, T., Edelman, S., Avidan, G., Itzhak, Y., Malach, R., 1999. Differential processing of objects under various viewing conditions in the human lateral occipital complex. *Neuron* 24, 187–203.
- Grill-Spector, K., Kushnir, T., Hendler, T., Malach, R., 2000. The dynamics of object-selective activation correlate with recognition performance in humans. *Nat. Neurosci.* 3, 837–843.
- Grill-Spector, K., Kourtzi, Z., Kanwisher, N., 2001. The lateral occipital complex and its role in object recognition. *Vision Res.* 41, 1409–1422.
- Harris, I.M., Miniussi, C., 2003. Parietal lobe contribution to mental rotation demonstrated with rTMS. *J. Cogn. Neurosci.* 15, 315–323.
- Harris, I.M., Egan, G.F., Sonkkila, C., Tochon-Danguy, H.J., Paxinos, G., Watson, J.D.G., 2000. Selective right parietal lobe activation during mental rotation: a parametric PET study. *Brain* 123, 65–73.
- Hasson, U., Harel, M., Levy, I., Malach, R., 2003. Large-scale mirror-symmetry organization of human occipito-temporal object areas. *Neuron* 37, 1027–1041.
- Heekeren, H.R., Marrett, S., Bandettini, P.A., Ungerleider, L.G., 2004. A general mechanism for perceptual decision-making in the human brain. *Nature* 431, 859–862.
- Holmes, C.J., Hoge, R., Collins, L., Woods, R., Toga, A.W., Evans, A.C., 1998. Enhancement of MR images using registration for signal averaging. *J. Comput. Assist. Tomogr.* 22, 324–333.
- Huk, A.C., Dougherty, R.F., Heeger, D.J., 2002. Retinotopy and functional subdivision of human areas MT and MST. *J. Neurosci.* 22, 7195–7205.
- Jordan, K., Wustenberg, T., Heinze, H.J., Peters, M., Jancke, L., 2002. Women and men exhibit different cortical activation patterns during mental rotation tasks. *Neuropsychologia* 40, 2397–2408.
- Just, M.A., Carpenter, P.A., Maguire, M., Diwadkar, V., McMains, S., 2001. Mental rotation of objects retrieved from memory: a functional MRI study of spatial processing. *J. Exp. Psychol. Gen.* 130, 493–504.
- Kanwisher, N., Wojciulik, E., 2000. Visual attention: insights from brain imaging. *Nat. Rev. Neurosci.* 1, 91–100.
- Kastner, S., Pinsk, M.A., 2004. Visual attention as a multilevel selection process. *Cogn. Affect. Behav. Neurosci.* 4, 483–500.
- Kirchhoff, B.A., Wagner, A.D., Maril, A., Stern, C.E., 2000. Prefrontal-temporal circuitry for episodic encoding and subsequent memory. *J. Neurosci.* 20, 6173–6180.
- Koshino, H., Carpenter, P.A., Keller, T.A., Just, M.A., 2005. Interactions between the dorsal and the ventral pathways in mental rotation: an fMRI study. *Cogn. Affect. Behav. Neurosci.* 5, 54–66.
- Kosslyn, S.M., Alpert, N.M., Thompson, W.L., Chabris, C.F., Rauch, S.L., Anderson, A.K., 1994. Identifying objects seen from different viewpoints. A PET investigation. *Brain* 117, 1055–1071.
- Kosslyn, S.M., DiGirolamo, G.J., Thompson, W.L., Alpert, N.M., 1998. Mental rotation of objects versus hands: neural mechanisms revealed by positron emission tomography. *Psychophysiology* 35.
- Kosslyn, S.M., Thompson, W.L., Wraga, M., Alpert, N.M., 2001. Imagining rotation by endogenous versus exogenous forces: distinct neural mechanisms. *NeuroReport* 12, 2519–2525.
- Kourtzi, Z., Bulthoff, H.H., Erb, M., Grodd, W., 2002. Object-selective responses in the human motion area MT/MST. *Nat. Neurosci.* 5, 17–18.
- Larsson, J., Heeger, D.J., 2006. Two retinotopic visual areas in human lateral occipital cortex. *J. Neurosci.* 26, 13128–13142.
- Lowe, D.G., 2000. Towards a computational model for object recognition in IT cortex. First IEEE International Workshop on Biologically Motivated Computer Vision, Seoul, Korea.
- Malach, R., Reppas, J.B., Benson, R.R., Kwong, K.K., Jiang, H., Kennedy, W.A., Ledden, P.J., Brady, T.J., Rosen, B.R., Tootell, R.B., 1995. Object-related activity revealed by functional magnetic resonance imaging in human occipital cortex. *Proc. Natl. Acad. Sci. U. S. A.* 92, 8135–8139.
- Metzler, J., Shepard, R.N., 1982. Transformational studies of the internal representation of three-dimensional objects. In: Shepard, R.N., Cooper, L.A. (Eds.), *Mental Images and Their Transformations*. MIT Press, Cambridge, MA, pp. 25–71.
- Milner, A.D., Goodale, M.A., 1993. Visual pathways to perception and action. *Prog. Brain Res.* 95, 317–337.
- Moore, C., Engel, S.A., 2001. Neural response to perception of volume in the lateral occipital complex. *Neuron* 29, 277–286.
- Morrone, M.C., Tosetti, M., Montanaro, D., Fiorentini, A., Cioni, G., Burr, D.C., 2000. A cortical area that responds specifically to optic flow, revealed by fMRI. *Nat. Neurosci.* 3, 1322–1328.

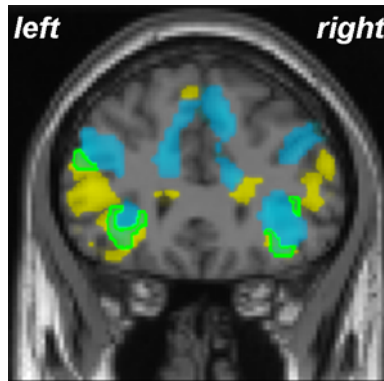
- Noppeney, U., Price, C.J., Penny, W.D., Friston, K.J., 2006. Two distinct neural mechanisms for category-selective responses. *Cereb. Cortex* 16, 437–445.
- Oldfield, R., 1971. The assessment and analysis of handedness: the Edinburgh inventory. *Neuropsychologia* 9, 97–113.
- Owen, A.M., Stern, C.E., Look, R.B., Tracey, I., Rosen, B.R., Petrides, M., 1998. Functional organization of spatial and nonspatial working memory processing within the human lateral frontal cortex. *Proc. Natl. Acad. Sci. U. S. A.* 95, 7721–7726.
- Petit, L., Clark, V.P., Ingeholm, J., Haxby, J.V., 1997. Dissociation of saccade-related and pursuit-related activation in human frontal eye fields as revealed by fMRI. *J. Neurophysiol.* 77, 3386–3390.
- Podzebenko, K., Egan, G.F., Watson, J.D., 2002. Widespread dorsal stream activation during a parametric mental rotation task, revealed with functional magnetic resonance imaging. *NeuroImage* 15, 547–558.
- Podzebenko, K., Egan, G.F., Watson, J.D., 2005. Real and imaginary rotary motion processing: functional parcellation of the human parietal lobe revealed by fMRI. *J. Cogn. Neurosci.* 17, 24–36.
- Postle, B.R., 2006. Working memory as an emergent property of the mind and brain. *Neuroscience* 139, 23–38.
- Richter, W., Somorjai, R., Summers, R., Jarnasz, M., Menon, R.S., Gati, J.S., Georgopoulos, A.P., Tegeler, C., Ugurbil, K., Kim, S.G., 2000. Motor area activity during mental rotation studied by time-resolved single-trial fMRI. *J. Cogn. Neurosci.* 12, 310–320.
- Sasaki, Y., Vanduffel, W., Knutsen, T., Tyler, C., Tootell, R., 2005. Symmetry activates extrastriate visual cortex in human and nonhuman primates. *Proc. Natl. Acad. Sci. U. S. A.* 102, 3159–3163.
- Schluppeck, D., Glimcher, P., Heeger, D.J., 2005. Topographic organization for delayed saccades in human posterior parietal cortex. *J. Neurophysiol.* 94, 1372–1384.
- Seurinck, R., Vingerhoets, G., Vandemaele, P., Deblaere, K., Achten, E., 2005. Trial pacing in mental rotation tasks. *NeuroImage* 25, 1187–1196.
- Shepard, R.N., Cooper, L.A., 1982. *Mental images and their transformations*. MIT Press, Cambridge, MA.
- Shikata, E., Hamzei, F., Glauche, V., Koch, M., Weiller, C., Binkofski, F., Buchel, C., 2003. Functional properties and interaction of the anterior and posterior intraparietal areas in humans. *Eur. J. Neurosci.* 17, 1105–1110.
- Silver, M.A., Ress, D., Heeger, D.J., 2005. Topographic maps of visual spatial attention in human parietal cortex. *J. Neurophysiol.* 94, 1358–1371.
- Stern, C.E., Owen, A.M., Look, R.B., Tracey, I., Rosen, B.R., Petrides, M., 2000. Activity in ventrolateral and mid-dorsolateral prefrontal cortex during non-spatial visual working memory processing: evidence from functional magnetic resonance imaging. *NeuroImage* 11, 392–399.
- Sugio, T., Inui, T., Matsuo, K., Matsuzawa, M., Glover, G.H., Nakai, T., 1999. The role of the posterior parietal cortex in human object recognition: a functional magnetic resonance imaging study. *Neurosci. Lett.* 276, 45–48.
- Talairach, J., Tournoux, P., 1988. *Co-Planar Stereotaxic Atlas of the Human Brain*. Thieme, New York.
- Tanaka, K., 2003. Columns for complex visual object features in the inferotemporal cortex: clustering of cells with similar but slightly different stimulus selectivities. *Cereb. Cortex* 13, 90–99.
- Tarr, M.J., 1995. Rotating objects to recognize them: a case study on the role of viewpoint dependency in the recognition of three-dimensional objects. *Psychon. Bull. Rev.* 2, 55–82.
- Tarr, M.J., Pinker, S., 1989. Mental rotation and orientation-dependence in shape recognition. *Cogn. Psychol.* 21, 233–282.
- Tarr, M.J., Pinker, S., 1990. When does human object recognition use a viewer-centered reference frame? *Psychol. Sci.* 1, 253–256.
- Tootell, R.B., Hadjikhani, N., Hall, E.K., Marrett, S., Vanduffel, W., Vaughan, J.T., Dale, A.M., 1998. The retinotopy of visual spatial attention. *Neuron* 21, 1409–1422.
- Tsao, D.Y., Vanduffel, W., Sasaki, Y., Fize, D., Knutsen, T.A., Mandeville, J.B., Wald, L.L., Dale, A.M., Rosen, B.R., Van Essen, D. C., Livingstone, M.S., Orban, G.A., Tootell, R.B., 2003. Stereopsis activates V3A and caudal intraparietal areas in macaques and humans. *Neuron* 39, 555–568.
- Tumblin, O.H., 1997. A double dissociation between knowledge of object identity and object orientation. *Neuropsychologia* 35, 567–570.
- Tumblin, O.H., McCarthy, R.A., 1996. When is a view unusual? A single case study of orientation-dependent visual agnosia. *Brain Res. Bull.* 40, 497–502.
- Tumblin, O.H., Beschin, N., DellaSala, S., 1997a. Agnosia for object orientation: implications for theories of object recognition. *Neuropsychologia* 35, 153–163.
- Tumblin, O.H., Carey, D.P., McCarthy, R.A., 1997b. The neuropsychology of object constancy. *J. Int. Neuropsychol. Soc.* 3, 288–298.
- Ungerleider, L.G., Haxby, J.V., 1994. ‘What’ and ‘where’ in the human brain. *Curr. Opin. Neurobiol.* 4, 157–165.
- Van Oostende, S., Sunaert, S., Van Hecke, P., Marchal, G., Orban, G.A., 1997. The kinetic occipital (KO) region in man: an fMRI study. *Cereb. Cortex* 7, 690–701.
- Vanrie, J., Beatse, E., Wagemans, J., Sunaert, S., Van Hecke, P., 2002. Mental rotation versus invariant features in object perception from different viewpoints: an fMRI study. *Neuropsychologia* 40, 917–930.
- Vincent, J.L., Snyder, A.Z., Fox, M.D., Shannon, B.J., Andrews, J.R., Raichle, M.E., Buckner, R.L., 2006. Coherent spontaneous activity identifies a hippocampal–parietal memory network. *J. Neurophysiol.* 96, 3517–3531.
- Warrington, E.K., 1982. Neuropsychological studies of object recognition. *Philos. Trans. R. Soc. London, B Biol. Sci.* 298, 15–33.
- Wig, G.S., Grafton, S.T., Demos, K.E., Kelley, W.M., 2005. Reductions in neural activity underlie behavioral components of repetition priming. *Nat. Neurosci.* 8, 1228–1233.
- Worsley, K.J., Marrett, S., Neelin, P., Vandal, A.C., Friston, K.J., Evans, A. C., 1996. A unified statistical approach for determining significant signals in images of cerebral activation. *Hum. Brain* 4.



Supplemental Figure 5. (A) Mental rotation ROI volumes. These ROIs were defined based on previously published coordinates of mental rotation areas (Barnes et al., 2000; Gauthier et al., 2002; Jordan et al., 2002; Kosslyn et al., 1998; Kosslyn et al., 2001; Podzebenko et al., 2002; Vanrie et al., 2002) to more precisely define overlap between object-sensitive regions and occipitoparietal mental rotation areas: DF1 (dark blue) and vcIPS (DF2; cyan light blue). The mental rotation ROI of caudal IPS (cIPS; or IPS2) is also shown (white). (B) Object-sensitive ROI volumes. These ROIs were defined based on previously published coordinates of object-sensitive areas (Grill-Spector et al., 2000; Hasson et al., 2003) to more precisely define common regions between tasks: dorsal foci of DF2 (cyan [light] blue) and DF1 (dark blue), DOT composed of the DOT-LOS (yellow) and DOT-ITS (green), VOT composed of VOT-pFs (red) and VOT-CoS (magenta purple).



Supplemental Figure 6. SPM for activation (Intact Object > Scrambled) in the medial temporal lobe bilaterally during the object-decision task at  $pFDR < .05$  overlaid on a sagittal slice in the left hemisphere ( $x = -27$ ) and a coronal slice ( $y = -20$ ) of an individual canonical MNI brain. Scale shows corresponding  $t$ -values. Arrows point to the hippocampus.



Supplemental Figure 7. SPM for mental rotation (blue) overlaid on the SPM for object-decision (yellow) at uncorrected  $p < .05$ , both of which are overlaid on a coronal slice ( $y = 30$ ) of an individual canonical MNI brain. Overlapping regions of the anterior part of ventrolateral prefrontal cortex (VLPFC; BA 45/47/12) were activated during both mental rotation and object-decision (overlapping voxels in green with green stroke), but most of the mental rotation activation did not overlap with the object-decision activation.